

## Research on Silicon Photomultipliers for various applications

---

### **Oleksandr Starodubtsev**<sup>1</sup>

*Universita degli Studi di Firenze, INFN sezione di Firenze  
Via Bruno Rossi 1, Sesto Fiorentino, Florence, Italy  
E-mail: Oleksandr.Starodubtsev@fi.infn.it*

### **Oscar Adriani**

*Universita degli Studi di Firenze, INFN sezione di Firenze  
Via Bruno Rossi 1, Sesto Fiorentino, Florence, Italy  
E-mail: adriani@fi.infn.it*

### **Mirko Brianzi**

*INFN sezione di Firenze  
Via Bruno Rossi 1, Sesto Fiorentino, Florence, Italy*

### **Guido Castellini**

*IFAC-CNR – Firenze  
Via Madonna del Piano, 10, Sesto Fiorentino, Florence, Italy*

### **Roberto Ciaranfi**

*INFN sezione di Firenze  
Via Bruno Rossi 1, Sesto Fiorentino, Florence, Italy*

### **Raffaello D'Alessandro**

*Universita degli Studi di Firenze, INFN sezione di Firenze  
Via Bruno Rossi 1, Sesto Fiorentino, Florence, Italy  
E-mail: candi@fi.infn.it*

### **Enrico Scarlini**

*Universita degli Studi di Firenze, INFN sezione di Firenze  
Via Bruno Rossi 1, Sesto Fiorentino, Florence, Italy*

### **Anna Vinattieri**

*Universita degli Studi di Firenze  
Via Bruno Rossi 1, Sesto Fiorentino, Florence, Italy  
E-mail: vinattieri@fi.infn.it*

---

<sup>1</sup> Speaker

The silicon photomultiplier is a novel semiconductor photo sensor which is operated in Geiger mode. It has high quantum efficiency, wide spectral range, low noise coupled to high gains, and fast time response. In the last few years, Silicon Photomultipliers (SiPMs) have become very popular in the detector research community because of these promising new features. Our group is currently evaluating and designing new devices for applications ranging from high energy physics and astroparticle physics, to earth imaging and gas and plasma spectroscopy. In this work device signal and current characterizations performed at various temperatures are presented. We have used fast laser pulsing to ascertain the time characteristics of the devices. A comparison between custom and commercially available devices is also made.

*10th International Conference on Large Scale Applications and Radiation Hardness of Semiconductor Detectors  
Firenze, Italy  
July 6-8, 2011*

## 1. Introduction

A silicon photomultiplier (SiPM) consists of an array of small independent avalanche photodiodes (pixels). On the rear side they are connected in parallel through the substrate, while on the top side they are equipped with polysilicon quenching resistors and connected to a single readout line. The operation voltage of the SiPM is a few volts above breakdown voltage, so that any photoelectron in a single pixel starts an avalanche discharge in that pixel.

Full characterization of the SiPM can be divided in three stages: static, dynamic and optical characterization. Static characterization includes forward and reverse current (IV) and capacitance (CV) measurements. Dynamic or signal characterization includes dark count, gain, after pulse probability, optical crosstalk measurements and temporal characterization. Optical characterization includes spectral sensitivity and photon detection efficiency measurements.

## 2. Experimental Procedure

### 2.1 Measurement Set-Up

All static and most dynamic characterizations must be done in absolute darkness. To perform this characterization a dedicated experimental set-up was developed. The set-up includes a light tight box with a copper support for the SiPM under test, which provides not only temperature control, but also electrical and optical connection to the device. For IV and CV measurements an HP 4142B and an HP 4284 instruments have been used. To perform signal characterization we have used a LeCroy SDA 760Zi oscilloscope (bandwidth - 6 GHz, Sample Rate - 40 GS/s) and a custom current preamplifier (gain  $\sim 10$ , bandwidth  $\sim 2$  GHz). For temporal characterization a fast laser pulse (frequency - 76 MHz, single pulse length - 4 ps, wavelength - 600 nm) and other ancillary equipment have been used.

### 2.2 The SiPM Devices

The data shown in this paper refer to the two following devices under test. The first one is a SiPM by FBK-IRST. This device has been packaged and bonded in our laboratory. We have used an opened TO case as package. The FBK-IRST SiPM has 292 cells with dimension  $70 \times 70$  micron<sup>2</sup> with a total active area of  $\sim 1.54$  mm<sup>2</sup>. A SiPM by Hamamatsu has been used as a benchmark. This is a standard Hamamatsu device S10362-11-050U series in its metal package. It has 400 cells with dimension  $50 \times 50$  micron<sup>2</sup> and its total active area is 1 mm<sup>2</sup>.

## 3. Static characterization

### 3.1 Forward IV measurements

Results on two important SiPM characteristics can be obtained from forward IV measurements: contact quality and quenching resistance values. Forward IV curves for the FBK device are shown in Fig.1. Curve clearly shows two different behaviours. For a bias voltage below 0.6 V the total current is determined by diode equivalent resistance and has an exponential growth. In the region above 0.6 V the current becomes limited by quenching

resistance and has a linear behavior. The slope of the linear fit in this area (red lines) gives us a total resistance of all quenching resistors connected in parallel. One can calculate the individual quenching resistor value dividing the number of cells by the slope coefficient. This measurement gives 650 k $\Omega$  for FBK and 129 k $\Omega$  for Hamamatsu respectively (see Tab.1.).

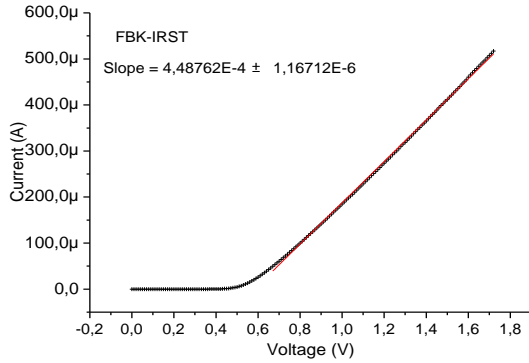


Fig.1. Forward IV

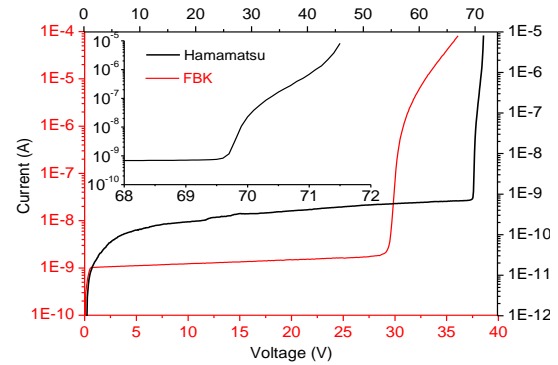


Fig.2. Reverse IV

### 3.2 Reverse IV measurements

The reverse IV curves also give important information about the functionality of the SiPM under test. First, the breakdown voltage can be determined very clearly. From the curves plotted on Fig.2 one can see that  $V_{BD}$  is 29.25 V for the FBK SiPM and 69.7 V for the Hamamatsu one (see Tab.1.). The procedure is based on the fact that before breakdown the surface current constitutes the main component of the total current [1]. After breakdown the total current is given by the volume current multiplied by the gain. The current behaviour after breakdown can be explained by considering the dynamics of SiPMs [2].

The second important parameter is the operational range. The total current after breakdown can be fitted with a parabolic function. However, as can be seen from the inset of Fig.2, the parabolic behaviour of the current stops above  $\sim 71.5$  V, a voltage that can be interpreted as the end of its working range for the SiPM by Hamamatsu. For the FBK device, the parabolic behavior of the current is maintained up to 36 V, the maximum applied reverse voltage, and no hint of deviation is observed. Taking in account the two  $V_{BD}$  values we can calculate the working range for each device which for FBK is larger than 7 V and for Hamamatsu is  $\sim 1.5$  V (see Tab.1.).

Knowing the gain for one SiPM, it is possible to calculate the dark count rate from the IV measurements. Supposing that the total current after breakdown is the average charge flowing through the SiPM, in the ideal case this would be given by the product of a single pulse charge and the number of pulses per second [2]. The charge of one pulse is given by the electron charge times the gain value. The number of pulses per second (dark count rate) can thus be determined. An example of this kind of calculations will be shown in section 4.2 where the gain of the devices is inferred from the dark count rate and IV curves.

### 3.3 Temperature dependence

Knowledge of the effects of temperature on our devices is very important because of the effect on the dark count rate due to carrier thermal generation, as predicted by Shockley-Read-

Hall theory [3]. The temperature dependence of the breakdown voltage is also an important issue, leading to large gain variations even when using fixed bias voltages.

To investigate the temperature behaviour of the devices we have performed IV tests at different temperatures in the range from  $-5\text{ }^{\circ}\text{C}$  to  $20\text{ }^{\circ}\text{C}$ . Fig.3 shows the breakdown voltage versus temperature dependence for both devices. Both sensors show a linear dependence and the slope is about of  $0.05\text{ V}/^{\circ}\text{C}$ . The dark count dependence will be shown in section 4 along with its dependence on the reverse bias voltage.

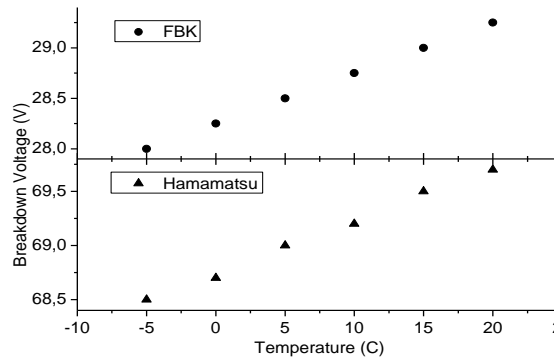


Fig.3. Temperature dependence

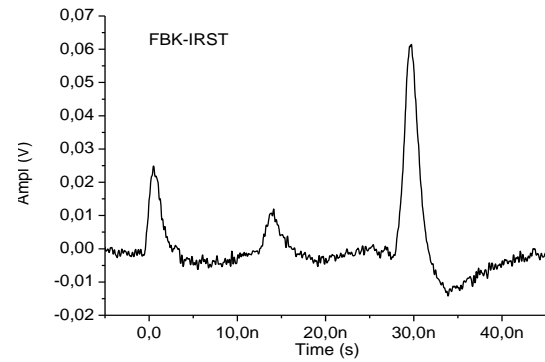


Fig.4. Typical signal of SiPM

## 4. Signal characterization

The electrical signal from a SiPM has a very fast leading edge determined by the avalanche propagation and a slow exponential decay determined by the discharge of the cell capacitance through the quenching resistor.

From the waveform measurements we can determine the following characteristics: signal amplitude, rise time, noise and signal distortion.

Fig.4 shows a waveform from an FBK SiPM kept in total darkness. The FBK device has higher signal amplitude than the Hamamatsu one, which is consistent with the fact that the operating range is greater for FBK than for Hamamatsu device. For these measurements FBK was operated at an overvoltage of  $3\text{ V}$  while the Hamamatsu at  $0.5\text{ V}$ . Also the FBK has a lower noise level which can be explained by the higher value of quenching resistor (see Tab.1.). Measured rise time is the same for both SiPMs and is equal to  $550\text{ ps}$ . This value is very close to the preamplifier bandwidth limit, so probably this is not the real rise time but the limit given by the readout electronics. Signal distortion (negative overshoot on the trailing edge of the pulse) is seen from the signal shape. This overshoot is also caused by the preamplifier.

### 4.1 Dark counts

The electronic noise of SiPMs is negligibly small due to the very high gain, so the main source of noise is the dark rate (dark counts). Dark rate originates from charge carriers thermally created in the sensitive volume and limits the SiPM's single photon resolution. This dark rate is also very sensitive to temperature.

Fig. 5 shows dark count rates for both SiPMs measured at different over voltages and temperatures. The FBK SiPM shows a much higher dark rate that is compatible with what one could expect from the IV measurements. On the other hand the FBK device shows a linear

dependence with overvoltage up to 6 V, whereas the Hamamatsu SiPM shows this linearity only up to 2 V. Both devices show a good linear dependence on temperature in the range from 5 to 20 °C. At lower temperature the dependence is not as linear. The non linear behavior at low overvoltage (first sets of points) is due to measurements errors arising from the very low signal amplitude.

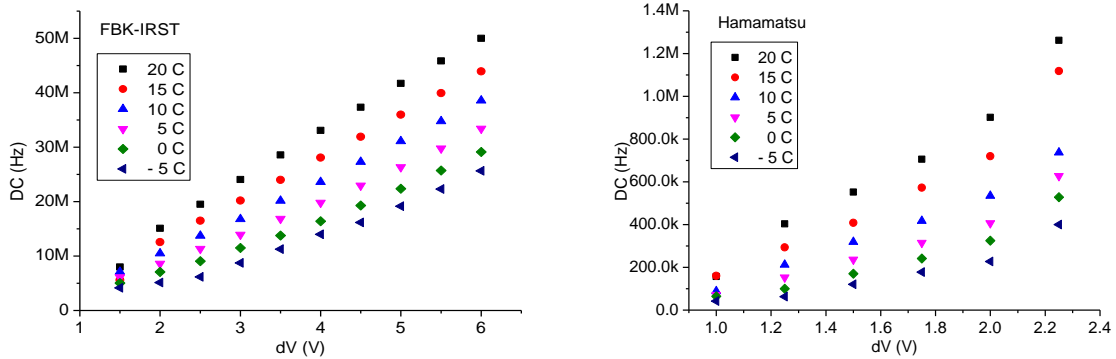


Fig.5. Dark counts for FBK-IRST and Hamamatsu

#### 4.2 Gain and optical crosstalk

The charge signal from the single pixel in a SiPM is determined by the charge accumulated on the pixel capacitance and is a product of this capacitance and over voltage value:  $C_p \times \Delta V$ . Typically  $C_p$  is about 50 fF and  $\Delta V$  is a few volts (see Tab.1.), so estimated signal should be of the order of 150 fC or  $10^6$  electrons.

The gain can be measured from the SiPMs charge spectrum. Fig.6 shows the spectrums for both the FBK and Hamamatsu SiPMs acquired at different over voltages with a 5 ns integration time. A preamplifier has been used for these measurements. Two types of peaks are presented in these spectrums. The first type is the principal peak with a higher rate. This is the peak given by one pixel and is equivalent to a one photoelectron signal. The second one with lower rate and a higher charge is a double photoelectron signal given by two pixels.

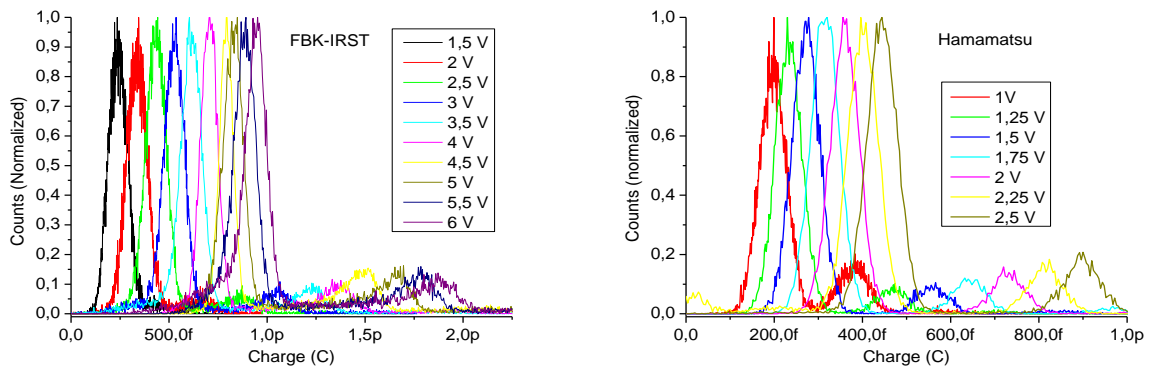


Fig.6. Charge spectrums for FBK-IRST and Hamamatsu (amplified by 10)

With the short integration times used, this type of structure is caused generally by optical crosstalk effects. The primary peak can be fitted by a Gaussian function. The centroid of this fit divided by electron charge gives the gain value (in electrons). The width ( $\sigma$ ) is the noise dominated by two contributions: readout system noise and gain fluctuations.

Gain dependences on overvoltage are shown in Fig.7 (a) (the preamplifier is taken into account). Both sensors have a good linearity (except last two points for FBK, caused probably to preamplifier saturation). To cross-check these gain measurements one can use the total current measurements (see section 3). Fig.7 (b) shows the gain values for FBK sensor measured and calculated using the fact that current after breakdown is given by the production of gain, dark count rate and electron charge. The calculated curve is a factor 10 higher than measured. The same difference has been observed for Hamamatsu sensor. This is the most probably due to the preamplifier limitations: low bandwidth and negative overshoot (see Fig.4.) The low bandwidth cut off the fast pulse component (front) and negative overshoot distorts slow components (tail). These effects give an underestimated measurement of collected charge.

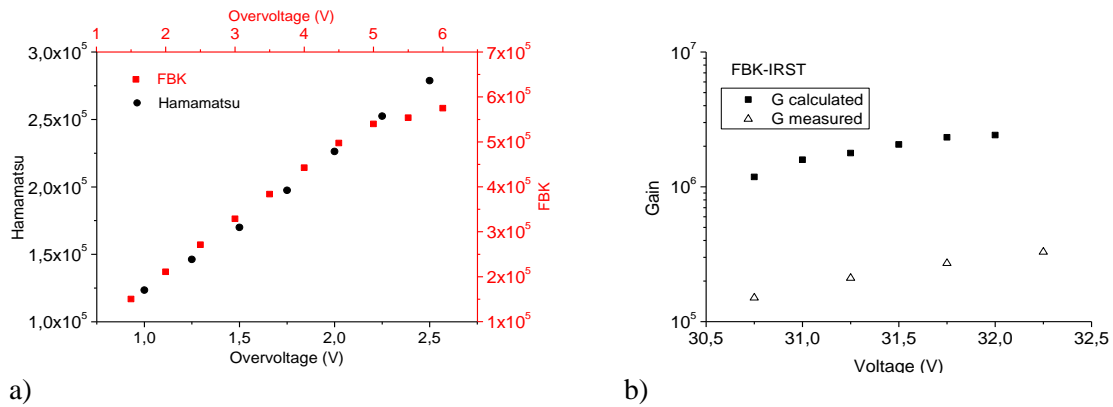


Fig.7. Gain

As stated above the charge spectra also provide information on the optical crosstalk of the device. This effect appears when some carriers from the avalanche in one pixel reach the sensitive volume of the near pixel and generate a spurious signal [4].

The secondary pulses in the spectra are caused mainly by this effect. In this case the relation between areas of the primary and secondary peaks gives the optical crosstalk value. Fig.8 shows the results for both devices under study.

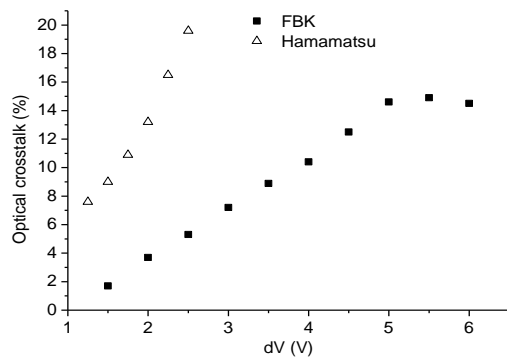


Fig.8. Optical crosstalk

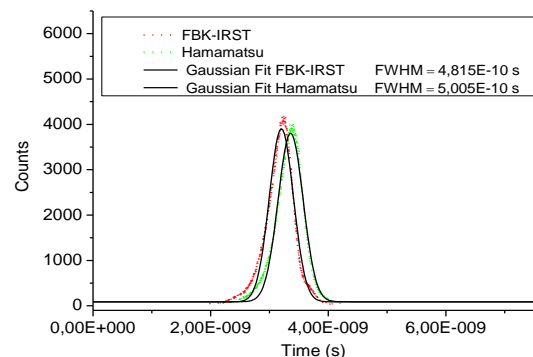


Fig.9. Temporal characterization

### 4.3 Temporal characterization

For the temporal characterization of the SiPMs the fast laser was used. This laser generates light pulses of 4 ps duration with a 76 MHz repetition frequency at 600 nm wavelength. The

time distribution of the signals in correspondence of the laser pulses was measured. The results are shown in Fig.9 where the spectra of both devices are fitted with Gaussians. The fits give a time resolution of 480 ps for the FBK and 500 ps for the Hamamatsu device. This time resolution again is very close to the preamplifier bandwidth limit.

## 5. Conclusions

Two SiPMs were extensively tested and characterized. One is a custom device from FBK, the second a commercial device from Hamamatsu. Measurements performed were: forward and reverse IV, CV, temperature dependence, dark count, gain, after pulse probability, optical crosstalk and temporal characterization. Summary of these measurements is on the Tab.1.

	$V_{BD}$ (V)	$\Delta V_{op}$ (V)	$I_{leak}$ (A)	$R_q$ k $\Omega$	C (pF)	Signal (mV)	Noise (mV)	Dark count (MHz)	Gain, max	Optical crosstalk	Rise time (ps)
FBK	29.25	> 6	$\leq 10e-4$	650	61	5-30	$\sim 2.5$	5 – 50	$5 \times 10^5$	2 – 15 %	$\sim 500$
HM	69.7	$\sim 2$	$\leq 10e-6$	129	36	3 – 8	$\sim 4.8$	0.05– 1.3	$2.8 \times 10^5$	7 – 20 %	$\sim 500$

Tab.1. Summary

The tested devices show significant differences in characteristics. The most important parameter, dark count rate, is much lower for the Hamamatsu SiPM. The device from FBK IRST has a higher gain, wider working region and lower optical crosstalk. Both SiPMs show very close time resolutions (given the set-up limitations).

The set-up developed for these measurements allows to perform static and dynamic characterizations. Results obtained are promising and bode well for future measurements on other devices. Future developments will involve increasing the preamplifier bandwidth and a modification to the cooling system for a more accurate temperature control with a capability of reaching down to  $-20^\circ\text{C}$ .

After-pulse measurements were difficult to perform with the existing set-up. First because of the lack of a dedicated triggering system, since for these measurements an advanced triggering and offline analysis is needed to select the “interesting” pulses. Second the preamplifier’s noise was too high to allow precise measurements.

## References

- [1] C. Piemonte et al, *Characterization of the First Prototypes of Silicon Photomultiplier Fabricated at ITC-irst*, IEEE Transactions On Nuclear Science, Vol.54, No.1, pp.236–244, 2007
- [2] C. Piemonte, *A new silicon photomultiplier structure for blue light detection*, Nucl. Instrum. Methods Phys. Res. A, vol.A568, pp.224–232, 2006.
- [3] S. M. Sze, *Physics of Semiconductor Devices* (John Wiley & Sons, NY) 1981.
- [4] A.Lacaita, F.Zappa, S.Bigliardi, M.Manfredi *On the bremsstrahlung origin of hot-carrier-induced photons in silicon devices*, IEEE Transactions Electron. Dev., 40, pp. 577-582, 1993